# Rhenium(I) Carbonyl Complexes of 2,4,6-Tris(2-pyridyl)-1,3,5-triazine (TPT). Rhenium(I)-Promoted Methoxylation of the Triazine Ring Carbon Atom in Dinuclear Rhenium Complexes

**Xiaoyuan Chen,[†] Frank J. Femia,[†] John W. Babich,[‡] and Jon A. Zubieta*[,†]**

Department of Chemistry, Syracuse University, Syracuse, New York 13244, and Biostream Inc., 160 Second Street, Cambridge, Massachusetts 02142

*Received April 25, 2000*

2,4,6-Tris(2-pyridyl)-1,3,5-triazine (TPT) bridged dinuclear rhenium(I) tricarbonyl halide complexes with the composition ($\mu$-TPT)[ReX(CO)$_3$]$_2$ (**3**, X = Cl; **4**, X = Br) can be made either by one-pot reaction of TPT with 2 equiv of [ReX(CO)$_5$] (X = Cl and Br) in chloroform or by reacting mononuclear [ReX(CO)$_3$(TPT)] $_2$ (**1**, X = Cl; **2**, X = Br) with an excess amount of [ReX(CO)$_5$]. Crystal data are as follows. **1**: monoclinic, $P2_1/c$, $a$ = 11.751(1) Å, $b$ = 11.376(1) Å, $c$ = 15.562(2) Å, $\beta$ = 103.584(2)°, $V$ = 2022.0(4) Å$^3$, $Z$ = 4. **2**: monoclinic, $P2_1/c$, $a$ = 11.896(1) Å, $b$ = 11.396(1) Å, $c$ = 15.655(1) Å, $\beta$ = 104.474(2)°, $V$ = 2054.9(3) Å$^3$, $Z$ = 4. **3:** triclinic, $P\bar{1}$, $a$ = 11.541(2) Å, $b$ = 12.119(2) Å, $c$ = 13.199(2) Å, $\alpha$ = 80.377(2)°, $\beta$ = 76.204(3)°, $\gamma$ = 66.826(2)°, $V$ = 1642.5(4) Å$^3$, $Z$ = 2. Crystals of **4** crystallized from acetone: triclinic, $P\bar{1}$, $a$ = 11.586(5) Å, $b$ = 12.144(5) Å, $c$ = 13.364(6) Å, $\alpha$ = 80.599(7)°, $\beta$ = 76.271(8)°, $\gamma$ = 67.158(8)°, $V$ = 1678.0(12) Å$^3$, $Z$ = 2. Crystals of **4′** are obtained from $CH_2Cl_2$−pentane solution: monoclinic, $C2/c$, $a$ = 17.555(4) Å, $b$ = 15.277(3) Å, $c$ = 13.093(3) Å, $\beta$ = 111.179(3)°, $V$ = 3274.0(12) Å$^3$, $Z$ = 4. By contrast, similar reactions in the presence of methanol yielded complexes with the composition [$\mu$-$C_3N_3$(OMe)(py)$_2$(pyH)][ReX(CO)$_3$]$_2$ (**5**, X = Cl; **6**, X = Br). Crystal data for **5**: monoclinic, $C2/c$, $a$ = 26.952(2) Å, $b$ = 16.602(1) Å, $c$ = 14.641(1) Å, $\beta$ = 116.147(1)°, $V$ = 5880.5(8) Å$^3$, $Z$ = 8. **6**: monoclinic, $C2/c$, $a$ = 27.513(3) Å, $b$ = 16.740(2) Å, $c$ = 14.837(2) Å, $\beta$ = 116.925(2)°, $V$ = 6092.8(10) Å$^3$, $Z$ = 8. An unusual metal-induced methoxylation at the carbon atom of the triazine ring of the bridging TPT ligand was observed. The nucleophilic attack of MeO$^-$ on C(3) results in a tetrahedral geometry around the carbon atom. Concomitantly, the uncoordinated pyridyl ring is protonated and rotated into a perpendicular orientation relative to the central $C_3N_3$ ring. Reaction of TPT with [NEt$_4$]$_2$[ReBr$_3$(CO)$_3$] in benzene−methanol resulted in an unexpected dinuclear complex **7**, with formulation [$\mu$-$C_3N_3$(OMe)(py)$_3$][Re(CO)$_3$][ReBr(CO)$_3$]. The methoxylated TPT ligand functions simultaneously as a tridentate and bidentate ligand with two *fac*-Re(CO)$_3^+$ cores. Crystal data for **7**: monoclinic, $P2_1/n$, $a$ = 12.114(1) Å, $b$ = 14.878(1) Å, $c$ = 15.807(1) Å, $\beta$ = 104.601(1)°, $V$ = 2756.9(3) Å$^3$, $Z$ = 4.

## Introduction

The ligand 2,4,6-tris(2-pyridyl)-1,3,5-triazine (TPT) has been widely used as an analytical reagent for various metal ions.[1−6] It's usually stable toward hydrolysis; concentrated sulfuric acid and temperatures above 150 °C are required for its hydrolytic reaction.[7] However, Lerner and Lippard[8,9] first reported that copper(II) promoted hydrolysis of the ligand to form a bis(2-pyridylcarbonyl)aminato chelate complex whose crystal structure was determined. On the basis of the Cu−N bond distances and angles at the carbonyl carbon atoms within the chelate ring, it was suggested that coordination of TPT induces an angular strain allowing nucleophilic attack at the carbon atoms of the triazine ring by the solvent, resulting in the formation of bis(2-pyridylcarbonyl)amido anions, which remain coordinated to Cu$^{2+}$, and free pyridine-2-carboxamide.[10,11] The hydrolytic reaction can be inhibited when N-donor tridentate ligands are bound to Cu$^{2+}$ as illustrated by the determination of the structure of [bis(2-pyridylcarbonyl)amido][2,4,6-tris(2-pyridyl)-1,3,5-triazine]copper(II) trifluoromethansulfonate.[12] The similar hydrolysis reaction was also observed upon reacting $RhCl_3 \cdot 3H_2O$ with TPT in refluxing ethanol−water.[13,14]

When TPT functions as a tridentate ligand, the coordination of a second metal to TPT is not usually observed due to deactivation of the triazine ring by the inductive effect of the first metal and as a result of steric interactions between the

* To whom correspondence should be addressed.
[†] Syracuse University.
[‡] Biostream, Inc.

(1) Collins, P.; Diehl, H.; Smith, G. F. *Anal. Chem.* **1959**, *31*, 1862.
(2) Embry, W. A.; Ayres, G. H. *Anal. Chem.* **1968**, *40*, 1499.
(3) Janmohamed, M. J.; Aryes, G. H. *Anal. Chem.* **1972**, *44*, 2263.
(4) Diehl, H.; Buchnana, E. B., Jr.; Smith, G. F. *Anal. Chem.* **1960**, *33*, 1117.
(5) Vagg, R. S.; Warrener, R. N.; Watton, E. C. *Aust. J. Chem.* **1969**, *22*, 141.
(6) Tsen, C. C. *Anal. Chem.* **1961**, *33*, 849.
(7) Smith, E. M.; Rapport, L. *S-Triazines and Derivatives*; Interscience: New York, 1959; p 163.
(8) Lerner, E. I.; Lippard, S. J. *J. Am. Chem. Soc.* **1976**, *98*, 5397.
(9) Lerner, E. I.; Lippard, S. J. *Inorg. Chem.* **1977**, *16*, 1546.
(10) Gil, V. M. S.; Gillard, R. D.; Williams, P. A.; Vagg, R. S.; Watton, E. C. *Transition Met. Chem.* (*Weinheim, Ger.*) **1979**, *4*, 14.
(11) Cantrarero, A.; Amigó, J. M.; Faus, J.; Julve, M.; Debaerdemaeker, T. *J. Chem. Soc., Dalton Trans.* **1988**, 2033.
(12) Faus, J.; Julve, M.; Amigó, J. M.; Debaerdemaeker, T. *J. Chem. Soc., Dalton Trans.* **1989**, 1681.
(13) Paul, P.; Tyagi, B.; Bhadbhade, M. M.; Suresh, E. *J. Chem. Soc., Dalton Trans.* **1997**, 2273.
(14) Paul, P.; Tyagi, B.; Bilakhiya, A. K.; Bhadbhade, M. M.; Suresh, E.; Ramachandraiah, G. *Inorg. Chem.* **1998**, *37*, 5733.

10.1021/ic000446g CCC: $20.00 
Published on Web 05/09/2001

hydrogen atoms and the metal ion.[15] However, recent investigations have found that this versatile ligand may also function as a bis-bidentate ligand.[5,16−19] The coordination of two low-valent metal ions to TPT leads to destabilization of the triazine ring by enhancing its electron deficiency; nucleophilic reaction may thus occur at the carbon atom on the triazine ring which is adjacent to uncoordinated pyridyl ring. The reaction of polymeric dicarbonyldichlororuthenium(II), $[Ru(CO)_2Cl_2]_n$, with TPT in methanol revealed a photoinduced methoxylation at the triazine ring and resulted in the formation of a dinuclear complex $\{\mu\text{-}C_3N_3(OMe)(py)_2(pyH)\}[Ru(CO)_2Cl_2]_2$. However, no methoxylation occurred when the same reaction was carried out in the dark.[17] The reaction of *cis*-$[M(bpy)_2Cl_2]$ (M = Ru(II) and Os(II)) with TPT in refluxing ethanol−water exhibited metal induced hydroxylation at C(3) on the triazine ring and the formation of dinuclear complexes of the composition $\{\mu\text{-}C_3N_3(OH)(py)_2(pyH)\}[M(bpy)_2]_2$.[19] Sufficient electrophilicity on C(3) and free movement of the attached pyridyl ring are responsible for the methoxylation or hydroxylation reaction.

We are interested in exploring the rhenium(I) tricarbonyl halide complexes of N-donor heterocyclic molecules such as TPT because of their favorable excited-state and redox properties. Previous study has shown that TPT acts in a bidentate mode in the mononuclear complex $[ReCl(CO)_3(TPT)]$.[18] This TPT-based product behaves as a bidentate metalloligand when it reacts with another molecule of $[ReCl(CO)_5]$ to give a homodinuclear $[\{ReCl(CO)_3\}_2(TPT)]$ complex or reacts with $[M(hfac)_2]$ (M = Mn, Co, Cu) producing the heterobimetallic $[(CO)_3ClRe(TPT)M(hfac)_2]$ species. In the absence of structural confirmation, the author tentatively concluded that in methanol solution the binuclear Re−TPT−Re complex forms the species $[\{ReCl(CO)_3\}_2(TPT)]\cdot MeOH$, where a methoxide group seems to be interacting with the acidic triazine ring and the nitrogen atom of uncoordinated pyridyl group is protonated. Due to the versatility of the coordination modes of TPT with various metal ions under different reaction conditions, we concluded that a systematic synthetic study and structural determination of rhenium(I) tricarbonyl halide complexes of TPT would be most helpful to fully understand the complextion behavior of dinuclear rhenium(I) complexes. For this purpose we reinvestigated the reaction of TPT with 2 equiv of $[ReX(CO)_5]$, and of the mononuclear $[ReX(CO)_3(TPT)]$ complex with 1 equiv of $[ReX(CO)_5]$ in different solvent systems. In the absence of methanol, we were able to prepare dinuclear Re(I) complexes of intact TPT. However, substitution of methoxide at the TPT triazine ring occurred to yield $[\mu\text{-}C_3N_3(OMe)(py)_2(pyH)][ReX(CO)_3]_2$ (**5**, X = Cl; **6**, X = Br) when chloroform−methanol was used as solvent. This Re(I)-promoted methoxylation reaction is similar to that observed for $[Ru(CO)_2Cl_2]_n$. Even more striking, the reaction between $[NEt_4]_2[ReBr_3(CO)_3]$ and TPT in benzene−methanol yielded an unexpected complex with methoxylation on the carbon atom of the triazine ring adjacent to the uncoordinated pyridyl ring. The methoxylated TPT bridge functions simultaneously as a tridentate and bidentate ligand with two *fac*-$Re(CO)_3^+$ subunits. We herein report the synthesis and structural and spectroscopic characterization of a series of dinuclear rhenium(I) carbonyl complexes of TPT under different reaction conditions.

## Experimental Section

**General Methods.** The ligand 2,4,6-tris(2-pyridyl)-1,3,5-triazine (TPT), $[Re(CO)_5Cl]$, and $[Re(CO)_5Br]$ were purchased from the Aldrich Chemical Co. $[NEt_4]_2[ReBr_3(CO)_3]$ was prepared according to the literature method.[20] All organic solvents were of reagent grade and were purified by standard methods before use. IR spectra were recorded as KBr pellets with a Perkin-Elmer Series 1600 FT-IR spectrometer in the region of 500−4000 $cm^{-1}$ with polystyrene as reference. Elemental analyses for carbon, hydrogen, and nitrogen were carried out by Oneida Research Services, Whitesboro, NY. $^1H$ NMR spectra were recorded on a Bruker DPX 300 ($^1H$ 300.10 MHz) spectrometer; all peak positions are relative to TMS. The UV/vis spectra were recorded on a Hewlett-Packard 8452A diode array spectrophotometer.

**Synthesis of Mononuclear Complexes $[ReX(CO)_3(TPT)]$ (1, X = Cl; 2, X = Br).** The mononuclear rhenium complexes were prepared by a modification of the literature procedure described for **1**.[18] $[ReX(CO)_5]$ (0.1 mmol) and TPT (33 mg, 0.105 mmol) in dry chloroform (40 $cm^3$) were heated to reflux under an atmosphere of nitrogen for 3 h. After being cooled to room temperature, the solution was filtered and evaporated to dryness to give a bright-red residue. Recrystallization from methanol gave orange-red plates suitable for X-ray crystallography.

**$[ReCl(CO)_3(TPT)]$ (1).** Yield: 49 mg (79%). Anal. Calcd for $C_{21}H_{12}ClN_6O_3Re$: C, 40.81; H, 1.94; N, 13.60. Found: C, 40.93; H, 1.85; N, 13.47. IR (KBr; $\nu/cm^{-1}$): 2018, 1914, 1875. UV/vis ($CH_2Cl_2$; $\lambda_{max}$, nm ($\epsilon$)): 435 ($4.8 \times 10^3$). $^1H$ NMR ($\delta$ (ppm), DMSO-$d_6$): 9.19 (d, $J$ = 4.8 Hz, $H^6$), 9.14 (d, $J$ = 4.8 Hz, $H^3$), 8.97 (d, $J$ = 5.1 Hz, $H^{6''}$), 8.92−8.85 (m, $H^{6',3''}$), 8.52 (t, $J$ = 7.8 Hz, $H^4$), 8.25−8.15 (m, $H^{4,4',4''}$), 8.02 (t, $J$ = 7.8 Hz, $H^5$), 7.8−7.7 (m, $H^{5',5''}$).

**$[ReBr(CO)_3(TPT)]$ (2).** Yield: 55 mg (83%). Anal. Calcd for $C_{21}H_{12}BrN_6O_3Re$: C, 38.07; H, 1.81; N, 12.69. Found: C, 38.19; H, 1.78; N, 12.75. IR (KBr; $\nu/cm^{-1}$): 2018, 1908, 1877. UV/vis ($CH_3CN$; $\lambda_{max}$, nm ($\epsilon$)): 415 ($5.1 \times 10^3$). $^1H$ NMR ($\delta$ (ppm), DMSO-$d_6$): 9.16 (d, $J$ = 5.1 Hz, $H^6$), 9.11 (d, $J$ = 5.1 Hz, $H^3$), 8.93 (d, $J$ = 5.1 Hz, $H^{6''}$), 8.9−8.8 (m, $H^{6',3''}$), 8.47 (t, $J$ = 7.8 Hz, $H^4$), 8.2−8.1 (m, $H^{4,4',4''}$), 7.98 (t, $J$ = 7.8 Hz, $H^5$), 7.8−7.7 (m, $H^{5',5''}$).

**Synthesis of Dinuclear Complexes ($\mu$-TPT)$[ReX(CO)_3]_2$ (3, X = Cl; 4, X = Br).** To the orange-red $[ReX(CO)_3(TPT)]$ complex (0.05 mmol) dissolved in refluxing chloroform (50 $cm^3$) was added $[ReX(CO)_5]$ (0.07 mmol). The resulting mixture was refluxed for 5 h, whereupon the color changed from red to dark brown, and was left to cool at ambient temperature. The solution was filtered, and a dark-red solid precipitated upon addition of pentane (100 $cm^3$). Red needle crystals were separated by slow evaporation from acetone/hexanes. The complexes can also be prepared in comparable yields via one-pot synthesis by refluxing TPT with 2.5 equiv of $[ReX(CO)_5]$ in chloroform. See Scheme 1.

**($\mu$-TPT)$[ReCl(CO)_3]_2\cdot 2C_3H_6O$ (3).** Yield: 35 mg (67%). Anal. Calcd for $C_{30}H_{24}Cl_2N_6O_8Re_2$: C, 34.65; H, 2.31; N, 8.08. Found: C, 34.73; H, 2.26; N, 8.13. IR (KBr; $\nu/cm^{-1}$): 2024, 1918 (br), 1702. UV/vis ($CH_2Cl_2$; $\lambda_{max}$, nm ($\epsilon$)): 501 ($7.8 \times 10^3$). UV/vis (MeOH; $\lambda_{max}$, nm ($\epsilon$)): 457 ($7.6 \times 10^3$), 383 ($7.2 \times 10^3$), 333 (sh, $7.3 \times 10^3$). $^1H$ NMR ($\delta$ (ppm), DMSO-$d_6$): 9.19 (d, $J$ = 4.8 Hz, $H^{6,6'}$), 9.0−8.9 (m, $H^{3,3',6''}$), 8.35 (t, $J$ = 5.1 Hz, $H^{4,4'}$), 8.16 (t, $H^{4''}$), 7.99 (t, $J$ = 7.8 Hz, $H^{3'',5}$), 7.8−7.7 (m, $H^{5',5''}$), 2.09 (s, 12H, $CH_3$).

**($\mu$-TPT)$[ReBr(CO)_3]_2\cdot 2C_3H_6O$ (4).** Yield: 41 mg (72%). Anal. Calcd for $C_{30}H_{24}Br_2N_6O_8Re_2$: C, 31.41; H, 2.27; N, 7.33. Found: C, 31.52; H, 2.26; N, 7.40. IR (KBr; $\nu/cm^{-1}$): 2024, 1918 (br), 1702. UV/Vis ($CH_2Cl_2$; $\lambda_{max}$, nm ($\epsilon$)): 466 ($8.1 \times 10^3$). UV/vis (MeOH; $\lambda_{max}$, nm ($\epsilon$)): 463 ($7.9 \times 10^3$), 384 ($7.0 \times 10^3$), 335 (sh, $7.1 \times 10^3$). $^1H$ NMR ($\delta$ (ppm), DMSO-$d_6$): 9.18 (d, $J$ = 5.4 Hz, $H^{6,6'}$), 9.0−8.8 (m, $H^{3,3',6''}$), 8.32 (t, $J$ = 5.4 Hz, $H^{4,4'}$), 8.14 (t, $H^{4''}$), 7.93 (t, $J$ = 7.8 Hz, $H^{3'',5}$), 7.8−7.7 (m, $H^{5',5''}$), 2.08 (s, 12H, $CH_3$).

(15) Durharm, D. A.; Frost, G. H.; Hart, F. A. *J. Inorg. Nucl. Chem.* **1969**, *31*, 571.
(16) Halfpenny, J.; Small, R. W. H. *Acta Crystallogr., Sect. B: Struct. Crystallogr. Cryst. Chem.* **1982**, *B38*, 939.
(17) Thomas, N. C.; Foley, B. L.; Rheingold, A. L. *Inorg. Chem.* **1988**, *27*, 7, 3426.
(18) Granifo, J. *Polyhedron* **1999**, *18*, 1061.
(19) Paul, P.; Tyagi, B.; Bilakhiya, A. K.; Dastidar, P.; Suresh, E. *Inorg. Chem.* **2000**, *39*, 14.
(20) Alberto, R.; Egli, A.; Abram, U.; Hegetschweiler, K.; Gramlich, V.; Schubiger, P. A. *J. Chem. Soc., Dalton Trans.* **1994**, 2815.

**Scheme 1**

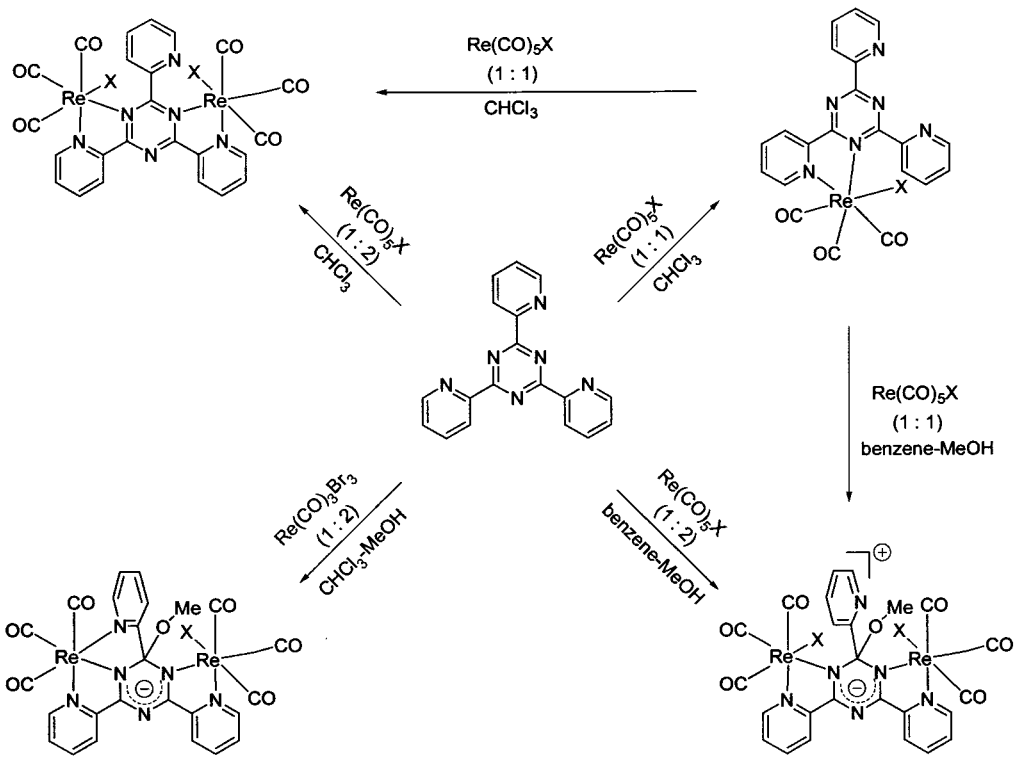


**Synthesis of the Methoxylated Dinuclear Complexes [$\mu$-$C_3N_3$-(OMe)(py)$_2$(pyH)][ReX(CO)$_3$]$_2$ (5, X = Cl; 6, X = Br).** A mixture of [ReX(CO)$_5$] (0.10 mmol) and TPT (0.04 mmol) in chloroform−methanol (50 cm$^3$, 3/1 v/v) was refluxed overnight and allowed to cool to room temperature. The resulting solution was filtered and concentrated to dryness. The red residue was redissolved in minimum amount of $CH_2Cl_2$. Slow addition of ice-cold methanol (20 cm$^3$) afforded a microcrystalline red solid which is sufficiently pure for analytical purposes. Crystals suitable for X-ray crytstallography were grown by diffusion of ethyl ether into solutions of the complexes in methanol.

**[$\mu$-$C_3N_3$(OMe)(py)$_2$(pyH)][ReCl(CO)$_3$]$_2$·MeOH (5).** Yield: 26 mg (65%). Anal. Calcd for $C_{26}H_{20}Cl_2N_6O_8Re_2$: C, 31.61; H, 2.03; N, 8.51. Found: C, 31.59; H, 2.11; N, 8.42. IR (KBr; $\nu$/cm$^{-1}$): 2024, 1902 (br), 1262. UV/vis ($CH_2Cl_2$; $\lambda_{max}$, nm ($\epsilon$)): 484 (8.0 × 10$^3$). UV/vis (MeOH; $\lambda_{max}$, nm ($\epsilon$)): 460 (7.7 × 10$^3$), 378 (7.3 × 10$^3$), 330 (sh, 7.9 × 10$^3$). $^1$H NMR ($\delta$ (ppm), $CDCl_3$): 9.19 (d, $J$ = 5.1 Hz, H$^{6,6'}$), 9.01 (d, $J$ = 5.1 Hz, H$^{3,3',6''}$), 8.32 (t, $J$ = 5.4 Hz, H$^{4,4'}$), 8.14 (t, H$^{4''}$), 7.99 (d, $J$ = 7.8 Hz, H$^{3''}$), 7.9−7.8 (m, H$^{5',5''}$), 7.73(m, H$^{5'}$), 3.85 (s, $CH_3O$), 3.47 (s, $CH_3OH$).

**[$\mu$-$C_3N_3$(OMe)(py)$_2$(pyH)][ReBr(CO)$_3$]$_2$·MeOH (6).** Yield: 30 mg (69%). Anal. Calcd for $C_{26}H_{20}Br_2N_6O_8Re_2$: C, 29.00; H, 1.86; N, 7.81. Found: C, 29.08; H, 1.91; N, 7.73. IR (KBr; $\nu$/cm$^{-1}$): 2022, 1910 (br), 1262. UV/vis ($CH_2Cl_2$; $\lambda_{max}$, nm ($\epsilon$)): 506 (8.3 × 10$^3$). UV/vis (MeOH; $\lambda_{max}$, nm ($\epsilon$)): 458 (8.1 × 10$^3$), 362 (7.5 × 10$^3$), 335 (sh, 7.7 × 10$^3$). $^1$H NMR ($\delta$ (ppm), DMSO-$d_6$): 9.17 (d, $J$ = 5.1 Hz, H$^{6,6'}$), 9.05−8.95 (m, $J$ = 5.1 Hz, H$^{3,3',6''}$), 8.55−8.50 (m, H$^{5'}$, pyH), 8.32 (t, $J$ = 5.4 Hz, H$^{4,4'}$), 8.14 (t, H$^{4''}$), 7.99 (d, $J$ = 7.8 Hz, H$^{3''}$), 7.9−7.8 (m, H$^{5',5''}$), 3.80 (s, $CH_3O$), 3.49 (s, $CH_3OH$).

**Synthesis of Dinuclear Complex [$\mu$-$C_3N_3$(OMe)(py)$_3$][Re(CO)$_3$]-[ReBr(CO)$_3$] (7).** To a solution of TPT (16 mg, 0.05 mmol) in benzene−methanol (100 cm$^3$, 5/1 v/v) was added [NEt$_4$]$_2$[ReBr$_3$(CO)$_3$] (82 mg, 0.11 mmol). The mixture was refluxed for 24 h, after which the solution was filtered and the solvent was evaporated under reduced pressure. The dark residue was washed (3 × 5 cm$^3$) with ice-cold methanol. Recrystallization from methylene chloride−methanol yielded compound **7** in 42% yield. Anal. Calcd for $C_{25}H_{15}BrN_6O_7Re_2$: C, 31.15; H, 1.56; N, 8.72. Found: C, 31.06; H, 1.63; N, 8.85. IR (KBr; $\nu$/cm$^{-1}$): 2025, 1915 (br), 1260. UV/vis ($CH_3CN$; $\lambda_{max}$, nm ($\epsilon$)): 462 (8.8 × 10$^3$). UV/vis (MeOH; $\lambda_{max}$, nm ($\epsilon$)): 458 (8.1 × 10$^3$), 379 (7.7 × 10$^3$). $^1$H NMR ($\delta$ (ppm), DMSO-$d_6$): 9.11 (d, $J$ = 5.1 Hz, 1H), 8.98 (m, 2H), 8.77 (m, 2H), 8.30 (m, 2H), 8.18 (m, 2H), 7.95 (d, $J$ = 7.8 Hz, 1H), 7.8−7.7 (m, 2H), 3.80 (s, $CH_3O$).

**X-ray Crystal Structure Determinations of 1−7 and 4′.** The selected crystals of **1**−**7** and **4′** were measured with a Siemens P4 diffractometer equipped with the SMART CCD system[21] and using graphite-monochromated Mo K$\alpha$ radiation ($\lambda$ = 0.071 073 Å). The data collection was carried out at 89(5) K. The data were corrected for Lorentz and polarization effects, and absorption corrections were made using SADABS.[22] Neutral atom scattering factors were taken from Cromer and Waber.[23] And anomalous dispersion corrections were taken from those of Creagh and McAuley.[24] All calculations were performed using SHELXL.[25] The structures were solved by direct methods,[26] and all of the non-hydrogen atoms were located from the initial solution. After location of all the initial non-hydrogen atoms in each structure, the models were refined against $F^2$, initially using isotropic and later anisotropic thermal displacement parameters, until the final value of $\Delta/\sigma_{max}$ was less than 0.001. At this point the hydrogen atoms were located from the electron density difference map and a final cycle of refinements was performed, until the final value of $\Delta/\sigma_{max}$ was again less than 0.001. No anomalies were encountered in the refinement of any of the structures. The relevant parameters for crystal data, data collection, structure solution, and refinement are summarized in Table 1, and important bond lengths and angles in Tables

2−5. A complete description of the details of the crystallographic methods is given in the Supporting Information.

(21) *SMART Software Reference Manual*; Siemens Analytical X-ray Instruments, Inc.: Madison, WI, 1994.
(22) Sheldrick, G. M. *SADABS: Program for Empirical Absorption Corrections*; University of Göttingen: Göttingen, Germany, 1996.
(23) Cromer, D. T.; Waber, J. T. *International Tables for X-ray Crystallography*; Kynoch: Birmingham, U.K., 1974; Vol. IV.
(24) Creagh, D. C.; McAuley, J. W. J. *International Tables for X-ray Crystallography*; Kluwer Academic: Boston, MA, 1992; Vol. C, Table 4.
(25) *SHELXL PC*; Siemens Analytical X-ray Instruments, Inc.: Madison, WI, 1990.
(26) *TeXan: Texray Structural Analysis Package (revised)*; Molecular Structure Corp: The Woodlands, TX, 1992.

**Table 1.** Summary of Crystallographic Data for Complexes **1**−**7** and **4′** [a]

| | **1** | **2** | **3** |
|---|---|---|---|
| empirical formula | $C_{21}H_{12}ClN_6O_3Re$ | $C_{21}H_{12}BrN_6O_3Re$ | $C_{24}H_{12}Cl_2N_6O_6Re_2{\cdot}2C_3H_6O$ |
| fw | 618.02 | 662.48 | 1039.86 |
| cryst size (mm) | 0.3 × 0.25 × 0.15 | 0.3 × 0.3 × 0.15 | 0.32 × 0.15 × 0.10 |
| cryst system | monoclinic | monoclinic | Triclinic |
| space group | $P2_1/c$ | $P2_1/c$ | $P\bar{1}$ |
| $a$ (Å) | 11.7506(13) | 11.8958(10) | 11.5407(15) |
| $b$ (Å) | 11.3757(12) | 11.3961(10) | 12.1186(16) |
| $c$ (Å) | 15.5617(17) | 15.6548(13) | 13.1992(18) |
| α (deg) | | | 80.377(2) |
| $\beta$ (deg) | 103.584(2) | 104.474(2) | 76.204(3) |
| $\gamma$ (deg) | | | 66.826(2) |
| $V$ (Å$^3$) | 2022.0(4) | 2054.9(3) | 1642.5(4) |
| $Z$ | 4 | 4 | 2 |
| $D_{calc}$ (Mg m$^{-1}$) | 2.030 | 2.141 | 2.115 |
| $F$(000) | 1184 | 1256 | 994 |
| $\mu$ (mm$^{-1}$) | 6.181 | 7.896 | 7.586 |
| final indices (2$\sigma$ data), R1 (wR2) | 0.0509 (0.1041) | 0.0437 (0.0831) | 0.0446 (0.0995) |
| all data, R1 (wR2) | 0.0959 (0.1194) | 0.0827 (0.0989) | 0.0795 (0.1228) |

| | **4** | **4** | **5** |
|---|---|---|---|
| empirical formula | $C_{24}H_{12}Br_2N_6O_6Re_2{\cdot}2C_3H_6OH_2O$ | $C_{23}H_{12}Br_2N_6O_6Re_2CH_2Cl_2{\cdot}0.5H_2O$ | $C_{25}H_{15}Cl_2N_6O_7Re_2{\cdot}CH_3OH$ |
| fw | 1146.77 | 1106.54 | 986.77 |
| cryst size (mm) | 0.3 × 0.3 × 0.15 | 0.3 × 0.2 × 0.1 | 0.38 × 0.17 × 0.08 |
| cryst system | triclinic | triclinic | monoclinic |
| space group | $P\bar{1}$ | $C2/c$ | $C2/c$ |
| $a$ (Å) | 11.586(5) | 17.555(4) | 26.952(2) |
| $b$ (Å) | 12.144(5) | 15.277(3) | 16.6019(12) |
| $c$ (Å) | 13.364(6) | 13.093(3) | 14.6405 |
| α (deg) | 80.599(7) | | |
| $\beta$ (deg) | 76.271(8) | 111.179(3) | 116.147(1) |
| $\gamma$ (deg) | 67.158(8) | | |
| $V$ (Å$^3$) | 1678.0(12) | 3274.0(12) | 5880.5(8) |
| $Z$ | 2 | 4 | 8 |
| $D_{calc}$ (Mg m$^{-1}$) | 2.226 | 2.261 | 2.229 |
| $F$(000) | 1076 | 2068 | 3720 |
| $\mu$ (mm$^{-1}$) | 9.651 | 10.042 | 8.468 |
| final indices (2$\sigma$ data), R1 (wR2) | 0.0587 (0.1489) | 0.0411 (0.1097) | 0.0509 (0.0930) |
| all data, R1 (wR2) | 0.0882 (0.1704) | 0.0527 (0.1220) | 0.1166 (0.1172) |

| | **6** | **7** |
|---|---|---|
| empirical formula | $C_{25}H_{16}Br_2N_6O_8Re_2{\cdot}CH_3OH$ | $C_{25}H_{15}BrN_6O_7Re_2$ |
| fw | 1075.69 | 963.74 |
| cryst size (mm) | 0.3 × 0.3 × 0.15 | 0.3 × 0.3 × 0.05 |
| cryst system | monoclinic | monoclinic |
| space group | $C2/c$ | $P2_1/n$ |
| $a$ (Å) | 27.513(3) | 12.1143(8) |
| $b$ (Å) | 16.7400(16) | 14.8778(11) |
| $c$ (Å) | 14.8373(15) | 15.8065(11) |
| $\beta$ (deg) | 116.925(2) | 104.601(1) |
| $V$ (Å$_3$) | 6092.8(10) | 2756.9(3) |
| $Z$ | 8 | 4 |
| $D_{calc}$ (Mg m$^{-1}$) | 2.345 | 2.322 |
| $F$(000) | 4008 | 1792 |
| $\mu$ (mm$^{-1}$) | 10.621 | 10.279 |
| Params refined | 394 | 370 |
| final indices (2$\sigma$ data), R1 (wR2) | 0.0477 (0.0884) | 0.0418 (0.0831) |
| all data, R1 (wR2) | 0.1206 (0.1161) | 0.0897 (0.1040) |

[a] Where R1 = $\Sigma(|F_o| - |F_c|)/\Sigma|F_o|$ and wR2 = $[\Sigma[w(F_o^2 - F_c^2)^2]/\Sigma[w(F_o^2)^2]]^{1/2}$.

## Results and Discussion

**Synthesis and Spectroscopic Characterization of the Complexes.** The mononuclear complexes $[ReX(CO)_3(TPT)]$ (**1**, X = Cl; **2**, X = Br) were prepared by treatment of $[ReX(CO)_5]$ with 2,4,6-tris(2-pyridyl)-1,3,5-triazine (TPT) in refluxing chloroform in the molar ratio 1:1. In the metal carbonyl stretching region of the infrared spectra, the complexes show three strong peaks consistent with a facial arrangement of the carbonyl groups,[27,28] which are assigned as A′(1), A″, and A′(2) vibrations, respectively.[29] This indicates that the TPT ligand is acting as a bidentate chelate ligand by substituting two equatorial carbonyl groups of the $[ReX(CO)_5]$ compound (Chart 1). In the COSY spectra of $[ReX(CO)_3(TPT)]$ complexes, there appear three sets of four resonances which may be assigned to different pyridyl groups. The resonances of the noncoordinated pyridyl ring C which appear at 8.93 ($H^{6''}$), 8.85 ($H^{3''}$), 8.14 ($H^{4''}$), and 7.71 ($H^{5''}$) ppm are essentially unshifted with respect to those of the uncomplexed ligand TPT. The chemical shifts of the remaining noncoordinated pyridyl ring B, adjacent to the rhenium(I) core, are similar to those of free ligand except for an upfield shift for $H^{3'}$ (8.47 ppm) relative to $H^{3''}$ (8.85 ppm). It is likely that the shielding of the $H^{3'}$ proton resulted as a consequence of its interaction with the coordinated $ReCl(CO)_3$ fragment. The coordinated A ring protons appear as the two low-field superimposed doublets at 9.16 ($H^6$) and 9.10 ($H^3$) ppm, coupled with the triplet at 7.98 ppm ($H^5$) and the overlapping multiplet at 8.17 ppm ($H^4$). The electronic spectra in the visible region of the $[ReX(CO)_3(TPT)]$ complexes show an intense and broad solvent dependent absorption that occurs at 415 nm in acetonitrile solution. With reference to previous spectroscopic work on rhenium(I) diimine systems,[30] this band is assigned as the d$\pi$(Re) → $\pi$*(TPT) metal-to-ligand charge transfer (MLCT) transition. This MLCT absorption band was found to red-shift with reducing polarity, i.e. from 405 nm (MeOH) to 442 nm ($CH_2Cl_2$) in complex **2**. According to the work on solvatochromism of rhenium(I) tricarbonyl diimine halide complexes by Wrighton and co-workers,[31] the Re−L (where L = diimine) bond distance would be shortened in the excited state due to an electrostatic attraction between the negatively charged L and the oxidized central metal. Thus, for excited states with charge separation [i.e., Re(I)−diimine → Re(II)−diimine(1−)], solvents of different polarity would stabilize the charge separated state to different extents, and polar solvents would be expected to stabilize the charge separated state more effectively than nonpolar solvents.[32]

**Chart 1**

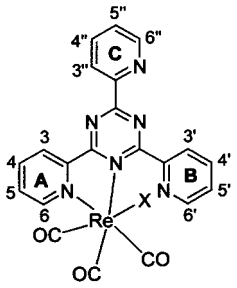


(27) Anderson, P. A.; Keene, F. R.; Horn, E.; Tiekink, E. R. T. *Appl. Organomet. Chem.* **1990**, *4*, 523.
(28) (28) Abel, E. W.; Orrell, K. G.; Osborne, A. G.; Pain, H. M.; Šik, V.; Hursthouse, M. B.; Malik, K. M. A. *J. Chem. Soc., Dalton Trans.* **1994**, 3441.
(29) Gamelin, D. R.; George, M. W.; Glyn, P.; Grevels, F.-W.; Johnson, F. P. A.; Klotzbucher, W.; Morrison, S. L.; Russell, G.; Schaffner, K.; Turner, J. J. *Inorg. Chem.* **1994**, *33*, 3246.
(30) Waterland, M. R.; Simpson, T. J.; Gordon, K. C.; Burrell, A. K. *J. Chem. Soc., Dalton Trans.* **1998**, 185.
(31) Fredericks, S. M.; Wrighton, M. S. *J. Am. Chem. Soc.* **1980**, *102*, 6166 and references therein.
(32) Dominey, R. N.; Hauser, B.; Hubbard, J.; Dunham, J. *Inorg. Chem.* **1991**, *30*, 4754.

**Chart 2**

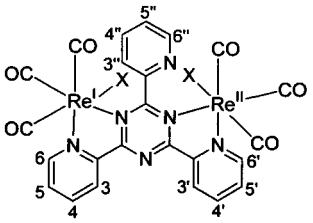

**A**

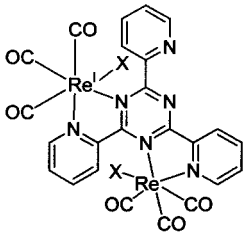

**B**

The mononuclear complex $[ReX(CO)_3(TPT)]$ reacts with $[ReX(CO)_5]$ in chloroform solution in the molar ratio 1:1 to give the dinuclear complexes ($\mu$-TPT)$[ReX(CO)_3]_2$ (**3**, X = Cl; **4**, X = Br). The IR spectrum contains one sharp and strong $\nu$(CO) absorption at 2025 $cm^{-1}$ and one broad and strong $\nu$-(CO) absorption at 1918 $cm^{-1}$, indicating cis CO groups. The IR band at 1702 $cm^{-1}$ indicates the presence of acetone in the complex, and the NMR peak at $\delta$ 2.10 ppm, together with analytical data, indicates the complexes recrystallize from acetone containing two acetone molecules. The aromatic region of the complex exhibits two sets (intensity ratio 2:1) of four resonances assignable to 12 pyridyl protons of the TPT ligand, which is expected for two magnetically equivalent coordinated pyridyl rings and one inequivalent pyridyl ring. The upfield shift of $H^{3'}$ with comparison to the free ligand is most probably a consequence of the interaction of the N atom of the unbound pyridyl ring with $H^{3'}$ or of ring-current effects from the unbound ring affecting $H^{3'}$.[33] Of the two possible configurations (Chart 2) for the complexes (**A** and **B**), structure **A** may be assigned on the basis of the crystal structure of the related complexes ($\mu$-TPT)$[ReX(CO)_3]_2$. Formation of **A** rather than the alternative **B** is most likely due to the steric interaction between $H^3$ and the metal in the latter case. No steric hindrance is present in **A** since the uncoordinated pyridyl ring is twisted out of the triazine ring. The electronic spectra of these complexes are also characterized by a broad low energy band in the visible region due most likely to a $d\pi \rightarrow \pi^*$(TPT) transition. The significant red-shifted (30−80 nm) absorption compared with those of the mononuclear species has been atributed mainly to the stabilization of the $\pi^*$ level of the bridging ligand of the monometallic species when it interacts with the second metal moiety, leading to enhanced $d\pi \rightarrow \pi^*$ overlap.[34,35] This effect lowers the HOMO−LUMO gap, which results in a low-energy shift of the MLCT bands in the dinuclear complexes. The high-energy band at 290 nm is a ligand-centered (LC) $\pi \rightarrow \pi^*$ transition.[36] While solutions of ($\mu$-TPT)$[ReX(CO)_3]_2$ complexes in $CH_2Cl_2$ are dark red, in methanol yellow solutions are observed. Similarly, electronic spectra of the complexes in MeOH are very different from those in methylene chloride. The broad band is replaced by two strong absorptions at ca. 460 and 380 nm. This unexpected dependence on solvent acidity of the spectra of these dinuclear Re(I) complexes of the intact TPT ligand compared to the monometallic complexes is presumably due to significant destabilization of the triazine ring, inducing partial positive charge on the TPT ligand on passing from the mononuclear to the bridged dinuclear complexes. Thus, the existence of an equilibrium between the acidic complex and the solvent molecule to form an acid−base adduct can be proposed. Electronic spectra similar to that obtained in MeOH were also observed in acetone, DMF, and DMSO.

**Scheme 2**

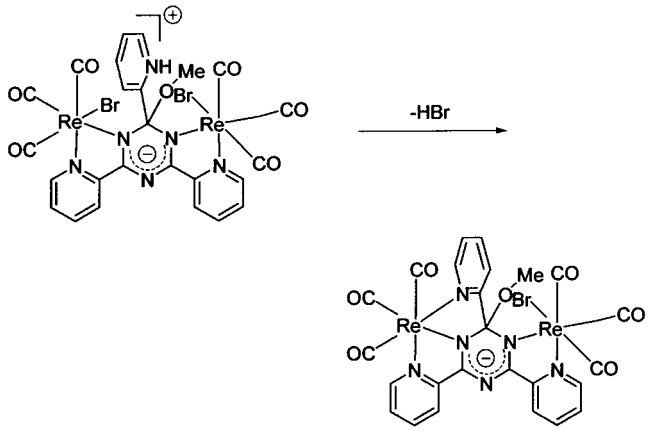


The dinuclear complexes with methoxylation at C(3) of the triazine ring were prepared by reaction of $[ReX(CO)_5]$ with TPT in the presence of methanol. Spectroscopic data for complexes **5** and **6** are given in the Experimental Section. The IR spectra of these complexes contain two strong $\nu$(CO) absorptions around 2020 and 1905 $cm^{-1}$, indicating cis CO groups. An additional band at 1262 $cm^{-1}$ (which is absent in the complexes **3** and **4**) may be assigned to the methoxy C−O−C. The $^1H$ NMR of **5** and **6** are very similar to those of **3** and **4** but contain an additional broad singlet at $\delta$ 8.55 ppm, which may be attributed to the proton on the uncoordinated pyridyl ring. A singlet at $\delta$ 3.85 ppm with integration of 3 protons is attributable to the methoxy methyl group. Electronic spectra of **5** and **6** in methanol are similar to those of complexes **3** and **4** but not identical. This is attributed to the existence of the acid−base equilibrium of the acidic methoxylated complex and methanol in these complexes.

Complex **7**, with the methoxylated TPT ligand acting simultaneously as a tridentate and bidentate ligand to Re(I) centers, was prepared by reaction of $[NEt_4]_2[ReBr_3(CO)_3]$ and TPT in 2:1 molar ratio in a mixture of benzene and methanol. The formation of complex of **6** was detected at an early stage of the reaction. Prolonged reaction times and higher reaction temperatures might be responsible for the elimination of one molecule of HBr and for overcoming the rotational barrier of the pyridyl ring attached to the $sp^3$-hydridized carbon C(3) upon formation of the complex **7** (Scheme 2). A significant downfield shift for all the protons of the metal-bound pyridyl rings is observed. Analysis of the variable-temperature $^1H$ NMR spectra of complex **7** (Supporting Information) in DMF-$d_7$ shows clearly the tumbling of the coordinated pyridyl ring at elevated temperatures. The increment of integration of resonances in the region 8.6−8.75 and 9.3−9.6 ppm and decrement of resonances in the region 7.8−8.55 and 8.85−9.1 ppm may suggest the fluxional behavior of the pyridyl ring which is almost perpendicular to the central $C_3N_3$ ring. It appears that this pyridyl ring could alternate between the two Re(I) centers in solution upon warming. This observation is consistent with the fact that complexes **1**, **2**, and **7** are not symmetrical and may have optical isomers in both the solid state and solution.

**Description of the Crystal Structures.** Selected bond distances and angles for complexes **1** and **2** are given in Table 2. A perspective view of complex **2** with the atom numbering is presented in Figure 1. These two complexes are very similar

(33) Maruyama, M.; Matsuzawa, H.; Kaizu, Y. *Inorg. Chim. Acta* **1995**, *237*, 159.
(34) Baiano, J. A.; Carlson, D. L.; Wolosh, G. M.; DeJesus, D. E.; Knowles, C. F.; Szabo, E. G.; Murphy, W. R. *Inorg. Chem.* **1990**, *29*, 2327.
(35) Rillema, D. P.; Mark, K. B. *Inorg. Chem.* **1982**, *21*, 3849.
(36) Berger, R. M.; Ellis, D. D., II. *Inorg. Chim. Acta* **1996**, *241*, 1.

**Table 2.** Selected Bond Lengths (Å) and Bond Angles (deg) for Complexes **1** and **2**

| | **1** | **2** |
|---|---|---|
| Bond Distances | | |
| Re(1)−C(19) | 1.915(8) | 1.890(8) |
| Re(1)−C(20) | 1.903(8) | 1.910(8) |
| Re(1)−C(21) | 1.924(9) | 1.927(8) |
| Re(1)−N(1) | 2.226(7) | 2.204(6) |
| Re(1)−N(4) | 2.191(7) | 2.185(6) |
| Re(1)−X(1) | 2.471(2) | 2.601(1) |
| Bond Angles | | |
| C(19)−Re(1)−C(20) | 87.4(3) | 87.5(3) |
| C(19)−Re(1)−C(21) | 88.2(4) | 87.8(4) |
| C(19)−Re(1)−N(1) | 171.3(3) | 171.1(3) |
| C(19)−Re(1)−N(4) | 96.9(3) | 96.8(3) |
| C(19)−Re(1)−X(1) | 94.5(2) | 93.6(2) |
| C(20)−Re(1)−C(21) | 87.6(4) | 87.7(4) |
| C(20)−Re(1)−N(1) | 95.9(3) | 96.3(3) |
| C(20)−Re(1)−N(4) | 97.4(3) | 97.2(3) |
| C(20)−Re(1)−X(1) | 178.0(2) | 178.6(2) |
| C(21)−Re(1)−N(1) | 99.9(3) | 100.3(3) |
| C(21)−Re(1)−N(4) | 173.0(3) | 173.4(3) |
| C(21)−Re(1)−X(1) | 93.0(3) | 93.1(2) |
| N(1)−Re(1)−N(4) | 74.8(2) | 74.8(2) |
| N(1)−Re(1)−X(1) | 82.1(2) | 82.4(2) |
| N(4)−Re(1)−X(1) | 81.9(2) | 81.9(2) |

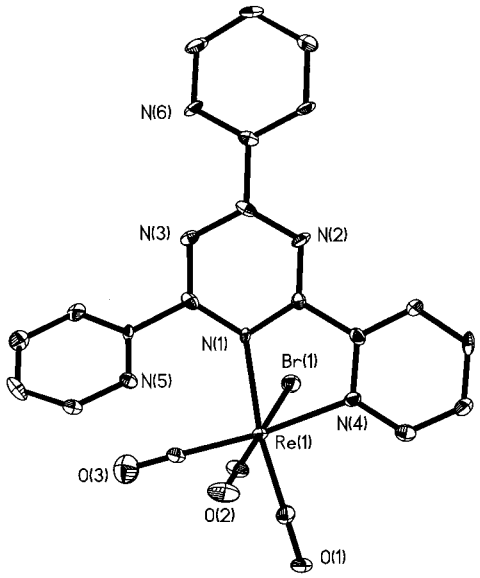


**Figure 1.** ORTEP view (50% probability) with atom-numbering scheme of complex **2**. Hydrogen atoms are omitted for clarity.

in structure, with the exception that the halide ligand for complex **1** is Cl while for **2** it is Br. The coordination geometry at the Re atom is a distorted octahedron with three carbonyl ligands arranged in the facial fashion. The trans angles at the $Re^{I}$ site are in the range 171.1(3)−178.6(2)°, showing a slight deviation from an ideal octahedral arrangement. The rhenium−nitrogen bond lengths are typical of rhenium(I) diimine systems [2.185(6)−2.226(7) Å], with the deviations attributable to small differences in the $\pi$-back-bonding.[37] The rhenium carbonyl bond lengths do not show any significant differences [1.890(8)−1.927(8) Å] and are consistent with those observed in similar complexes.[38] The N(1)−Re−N(4) angle of 74.8(2)° is significantly smaller than 90°, as a result of the small bite angle of the polypyridyl ligand. The ligand is distorted from planarity by steric interactions between the pyridyl rings. In complex **1**, the ring B [C(4)−C(5)−C(6)−C(7)−C(8)−N(6)] is rotated at an angle of 45.3° with respect to the triazine ring, 48.1° with respect to the coordinated pyridyl ligand ring A [C(14)−C(15)−C(16)−C(17)−C(18)−N(4)], and 40.8° with respect to ring C [C(4)−C(5)−C(6)−C(7)−C(8)−N(6)]. The coordinated pyridyl ring A is slightly twisted (9.0°) with respect to the triazine ring. Complex **2** showed very similar distortion geometry of the ligand. Ring B is rotated at an angle of 43.2° with respect to the triazine ring, 47.6° with respect to the coordinated pyridyl ring A, and 40.0° with respect to ring C. The coordinated ring A is twisted 8.4° from the triazine plane.

**Table 3.** Selected Bond Lengths (Å) and Bond Angles (deg) for Complexes **3**, **4**, and **4′**

| | **3** | **4** | **4′** |
|---|---|---|---|
| Bond Distances | | | |
| Re(1)−C(19) | 1.911(10) | 2.015(15) | 1.919(9) |
| Re(1)−C(20) | 1.925(10) | 1.909(12) | 1.907(8) |
| Re(1)−C(21) | 1.927(10) | 1.933(10) | 1.923(8) |
| Re(1)−N(1) | 2.210(8) | 2.217(9) | 2.180(6) |
| Re(1)−N(4) | 2.176(8) | 2.163(10) | 2.217(6) |
| Re(1)−X(1) | 2.483(2) | 2.615(2) | 2.606(1) |
| Re(2)−C(22) | 1.896(13) | 1.910(18) | |
| Re(2)−C(23) | 1.924(10) | 1.930(15) | |
| Re(2)−C(24) | 1.911(14) | 1.910(12) | |
| Re(2)−N(3) | 2.209(7) | 2.214(9) | |
| Re(2)−N(5) | 2.170(8) | 2.191(11) | |
| Re(2)−X(2) | 2.486(3) | 2.579(2) | |
| Bond Angles | | | |
| C(19)−Re(1)−C(20) | 90.7(4) | 92.6(5) | 89.8(4) |
| C(19)−Re(1)−C(21) | 90.2(4) | 92.5(5) | 90.4(4) |
| C(19)−Re(1)−N(1) | 93.9(3) | 92.7(4) | 95.2(3) |
| C(19)−Re(1)−N(4) | 94.2(3) | 92.2(5) | 95.2(3) |
| C(19)−Re(1)−X(1) | 175.1(3) | 174.5(4) | 177.4(3) |
| C(20)−Re(1)−C(21) | 86.9(3) | 87.8(5) | 86.4(3) |
| C(20)−Re(1)−N(1) | 102.9(3) | 102.0(4) | 95.9(3) |
| C(20)−Re(1)−N(4) | 174.6(3) | 174.5(4) | 169.8(3) |
| C(20)−Re(1)−X(1) | 90.9(3) | 90.0(3) | 92.7(3) |
| C(21)−Re(1)−N(1) | 169.3(3) | 168.8(4) | 174.0(3) |
| C(21)−Re(1)−N(4) | 95.3(3) | 94.6(4) | 102.4(3) |
| C(21)−Re(1)−X(1) | 94.5(3) | 92.4(3) | 90.4(2) |
| N(1)−Re(1)−N(4) | 74.5(3) | 75.2(3) | 74.9(2) |
| N(1)−Re(1)−X(1) | 81.3(2) | 82.1(2) | 83.9(2) |
| N(4)−Re(1)−X(1) | 84.0(2) | 85.0(2) | 82.3(2) |
| C(22)−Re(2)−C(23) | 91.0(5) | 89.8(7) | |
| C(22)−Re(2)−C(24) | 86.7(5) | 87.9(6) | |
| C(22)−Re(2)−N(3) | 94.6(5) | 94.7(5) | |
| C(22)−Re(2)−N(5) | 95.9(5) | 95.8(6) | |
| C(22)−Re(2)−X(2) | 178.1(4) | 178.8(4) | |
| C(23)−Re(2)−C(24) | 86.3(4) | 87.1(5) | |
| C(23)−Re(2)−N(3) | 100.7(3) | 100.1(4) | |
| C(23)−Re(2)−N(5) | 172.0(3) | 172.7(4) | |
| C(23)−Re(2)−X(2) | 89.8(3) | 90.0(4) | |
| C(24)−Re(2)−N(3) | 172.8(4) | 172.4(5) | |
| C(24)−Re(2)−N(5) | 98.1(4) | 97.9(5) | |
| C(24)−Re(2)−X(2) | 95.1(3) | 93.3(4) | |
| N(3)−Re(2)−N(5) | 74.7(3) | 74.7(4) | |
| N(3)−Re(2)−X(2) | 83.6(2) | 84.2(2) | |
| N(5)−Re(2)−X(2) | 83.2(2) | 84.3(2) | |

Selected bond distances and angles for complexes **3**, **4**, and **4′** are given in Table 3. A perspective view of complex **4** with the atom numbering is presented in Figure 2. In these complexes, the bridging TPT ligand functions as a bis-bidentate ligand to two rhenium(I) centers. One halide ligand, three carbonyl ligands, and a bidentate set of nitrogen donors from TPT form a distorted octahedral geometry around each metal ion. In the coordination sphere of Re(1), the least-squares plane through the atoms N(1), N(4), C(20), and C(21) (best plane) and in that of Re(2) the least-squares plane through the atoms N(3), N(5),

(37) Bardwell, D. A.; Barigelletti, F.; Cleary, R. L.; Flamigni, L.; Guardigli, M.; Jeffery, J. C.; Ward, M. D. *Inorg. Chem.* **1995**, *34*, 2438.
(38) Moya, S. A.; Guerrero, J.; Pastene, R.; Schmidt, R.; Sariego, R.; Sartori, R.; Sanz-Aparicio, J.; Fonseca, I.; Martinez-Ripoll, M. *Inorg. Chem.* **1994**, *33*, 2341.

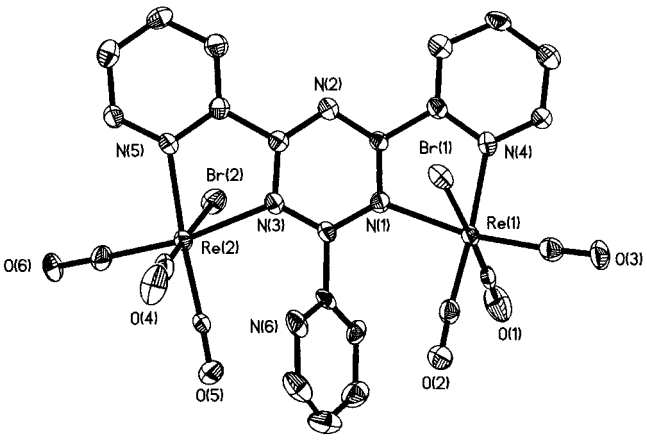


**Figure 2.** ORTEP view (50% probability) with atom-numbering scheme of complex **4**. Hydrogen atoms are omitted for clarity.

C(23), and C(24) (best plane) show very slight tetrahedral distortions (average deviation less than ±0.05 Å). In the chloride complex **3**, the Re(1) and Re(2) sites lie in the equatorial planes. However, the rhenium(I) sites in the bromide complex **4** project slightly from the equatorial planes, with average out-of-plane distances of 0.13 Å. The source of the distortion primarily reflects the acute ligand bite angles. The bite angles (average 74.8°) are significantly smaller than the ideal value of 90° because of the constraints imposed by the five-membered chelate rings. The ligand is distorted from planarity by steric interactions between the pyridyl rings. In complex **3**, the free pyridyl ligand [C(14)−C(15)−C(16)−C(17)−C(18)−N(6)] is rotated 64.7° with respect to the triazine ring to minimize the steric interactions with the coordination spheres on both sides of this ring. The pyridyl rings coordinated to Re(1) and Re(2) are tilted 10.9 and 11.3°, respectively, from the $C_3N_3$ triazine ring in the direction of the pyridyl ring bound at C(3).

Selected bond distances and angles for complexes **5** and **6** are given in Table 4. A perspective view of complex **6** with the atom numbering is given in Figure 3. The heterocyclic ligand functions as a bis-bidentate ligand to two rhenium atoms each coordinated to a nitrogen atom of the $C_3N_3$ triazine moiety and a pyridyl nitrogen atom. The complex contains a pseudo mirror plane perpendicular to the central $C_3N_3$ and containing the groups attached at C(3). The coordination sphere about the rhenium is slightly distorted from idealized octahedral geometry with two cis carbonyl groups in the chelation plane and the third carbonyl group and halide atom occupying the axial positions. An unprecedented methoxylation occurred at one of the carbon atoms (C(3)) of the triazine ring, forming tetrahedral geometry around C(3). The angles around C(3) are in the range of 108.0(8)−114.2(8)° (Table 4), which are close to the ideal tetrahedral value of 109.28°. The $C_3N_3$ ring C−N distances at C(3) are typical single-bond values (average 1.474(13) Å),[39] with the remaining four C−N distances narrowly spread in the double-bond range (average 1.332(13) Å). This latter value is similar to the mean bond distances reported in TPT complexes, e.g. averages of 1.36 Å for $Hg_2(CF_3CO_2)_4(TPT)$,[16] 1.35 Å for $[Ni(H_2O)_3(TPT{\bullet}HBr)]^{2+}$,[40] 1.33 Å for $[\mu\text{-}C_3N_3(OMe)(py)_2(pyH)][Ru(CO)_2Cl_2]_2$,[17] and 1.32 Å for $[\mu\text{-}C_3N_3(OH)(py)_2(pyH)][Os(bpy)_2]_2^{3+}$.[19] The methoxylated triazine ring is nonplanar. However, the five atoms N(1), N(2), N(3), C(1), and C(2) are approximately planar (average deviation ±0.017 Å for complex **5** and ±0.075 Å for complex **6**), supporting a pentadienide delocalized bonding mode. The deviations of C(3) from this least-squares plane are 0.312 and 0.168 Å for complexes **5** and **6**, respectively. The central $C_3N_3$ ring and the uncoordinated pyridyl ring are nearly perpendicularly oriented with an interplanar angle of 94.4° for complex **5** and 92.6° for complex **6**. The uncoordinated pyridyl ring is most likely the protonation site required to balance the negative charge induced by the pentadienide moiety. However, the crystal data were inadequate to positively identify the presence of the proton at N(6).

**Table 4.** Selected Bond Lengths (Å) and Bond Angles (deg) for Complexes **5** and **6**

| | **5** | **6** |
|---|---|---|
| Bond Distances | | |
| Re(1)−C(20) | 1.892(11) | 1.901(14) |
| Re(1)−C(21) | 1.918(14) | 1.914(14) |
| Re(1)−C(22) | 1.925(11) | 1.915(17) |
| Re(1)−N(1) | 2.178(8) | 2.214(9) |
| Re(1)−N(4) | 2.160(8) | 2.150(9) |
| Re(1)−X(1) | 2.491(3) | 2.641(2) |
| Re(2)−C(23) | 1.882(11) | 1.863(14) |
| Re(2)−C(24) | 1.925(11) | 1.895(14) |
| Re(2)−C(25) | 1.928(11) | 1.914(12) |
| Re(2)−N(2) | 2.176(8) | 2.176(9) |
| Re(2)−N(5) | 2.177(9) | 2.155(9) |
| Re(2)−X(2) | 2.485(3) | 2.621(2) |
| C(3)−N(1) | 1.480(13) | 1.453(15) |
| C(3)−N(2) | 1.467(13) | 1.499(14) |
| C(3)−C(14) | 1.522(14) | 1.557(16) |
| C(3)−O(7) | 1.414(12) | 1.420(14) |
| Bond Angles | | |
| C(20)−Re(1)−C( 21) | 88.3(5) | 89.1(5) |
| C(20)−Re(1)−C( 22) | 92.0(5) | 91.4(6) |
| C(20)−Re(1)−N( 1) | 166.9(4) | 166.8(4) |
| C(20)−Re(1)−N( 4) | 92.3(4) | 91.4(5) |
| C(20)−Re(1)−X( 1) | 91.4(4) | 89.7(4) |
| C(21)−Re(1)−C( 22) | 89.4(5) | 91.5(6) |
| C(21)−Re(1)−N( 1) | 104.0(4) | 103.4(5) |
| C(21)−Re(1)−N( 4) | 173.1(4) | 172.6(5) |
| C(21)−Re(1)−X( 1) | 89.1(4) | 88.1(5) |
| C(22)−Re(1)−N( 1) | 92.5(4) | 92.4(5) |
| C(22)−Re(1)−N( 4) | 97.5(4) | 95.8(4) |
| C(22)−Re(1)−X( 1) | 176.2(3) | 178.8(4) |
| N(1)−Re(1)−N(4) | 74.9(3) | 75.7(3) |
| N(1)−Re(1)−X(1) | 84.5(2) | 86.5(3) |
| N(4)−Re(1)−X(1) | 84.0(2) | 84.5(3) |
| C(23)−Re(2)−C( 24) | 91.2(5) | 90.0(6) |
| C(23)−Re(2)−C( 25) | 85.9(5) | 84.6(5) |
| C(23)−Re(2)−N( 2) | 170.7(4) | 171.4(5) |
| C(23)−Re(2)−N( 5) | 95.0(4) | 96.0(5) |
| C(23)−Re(2)−X( 2) | 92.9(4) | 92.0(4) |
| C(24)−Re(2)−C( 25) | 88.8(5) | 88.5(5) |
| C(24)−Re(2)−N( 2) | 91.0(4) | 92.8(4) |
| C(24)−Re(2)−N( 5) | 96.4(4) | 96.3(4) |
| C(24)−Re(2)−X( 2) | 175.6(3) | 177.7(3) |
| C(25)−Re(2)−N( 2) | 103.2(4) | 103.6(4) |
| C(25)−Re(2)−N( 5) | 174.6(4) | 175.2(4) |
| C(25)−Re(2)−X( 2) | 92.9(3) | 92.8(4) |
| N(2)−Re(2)−N(5) | 75.8(3) | 75.6(3) |
| N(2)−Re(2)−X(2) | 84.7(2) | 85.1(3) |
| N(5)−Re(2)−X(2) | 81.8(2) | 82.5(2) |
| O(7)−C(3)−N(2) | 110.6(9) | 108.0(10) |
| O(7)−C(3)−N(1) | 110.1(8) | 113.2(10) |
| N(2)−C(3)−N(1) | 114.2(8) | 113.2(9) |
| O(7)−C(3)−C(14) | 104.6(8) | 108.7(10) |
| N(2)−C(3)−C(14) | 108.0(8) | 108.7(10) |

A perspective view (ORTEP) of the complex **7** with the atom numbering is shown in Figure 4; selected bond distances and angles are given in Table 5. The molecular geometry of **7** is of considerable interest, as the methoxylated TPT compound

(39) Allen, F. H.; Kennard, O.; Watson, D. G.; Brammer, L.; Orpen, A. G.; Yalor, R. *J. Chem. Soc., Perkin Trans. 2* **1987**, 91.
(40) Barclay, G. A.; Vagg, R. S.; Watton, E. C. *Acta Crystallogr., Sect. B: Struct. Crystallogr. Cryst. Chem.* **1977**, *B33*, 3487.

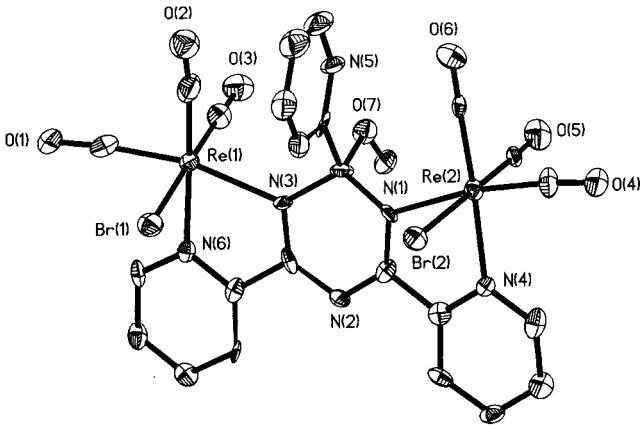


**Figure 3.** ORTEP view (50% probability) with atom-numbering scheme of complex **6**. Hydrogen atoms are omitted for clarity.

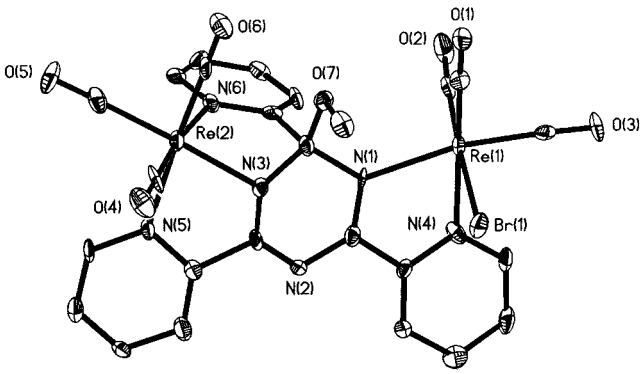


**Figure 4.** ORTEP view (50% probability) with atom-numbering scheme of complex **7**. Hydrogen atoms are omitted for clarity.

**Table 5.** Selected Bond Lengths (Å) and Bond Angles (deg) for Complex **7**

| Bond Distances | | | |
|---|---|---|---|
| Re(1)−C(24) | 1.900(11) | Re(2)−C(20) | 1.910(10) |
| Re(1)−C(23) | 1.909(12) | Re(2)−C(22) | 1.929(11) |
| Re(1)−C(25) | 1.915(9) | Re(2)−C(21) | 1.935(10) |
| Re(1)−N(4) | 2.192(8) | Re(2)−N(3) | 2.164(7) |
| Re(1)−N(1) | 2.217(6) | Re(2)−N(5) | 2.203(8) |
| Re(1)−Br(1) | 2.6250(11) | Re(2)−N(6) | 2.245(8) |
| C(3)−C(14) | 1.557(13) | C(3)−N(3) | 1.448(10) |
| C(3)−N(1) | 1.511(11) | C(3)−O(7) | 1.394(11) |
| **Bond Angles** | | | |
| C(24)−Re(1)−C(23) | 89.7(5) | C(20)−Re(2)−C(22) | 90.9(4) |
| C(24)−Re(1)−C(25) | 85.8(4) | C(20)−Re(2)−C(21) | 89.7(4) |
| C(23)−Re(1)−C(25) | 88.3(4) | C(22)−Re(2)−C(21) | 85.2(4) |
| C(24)−Re(1)−N(4) | 101.5(4) | C(20)−Re(2)−N(3) | 102.5(4) |
| C(23)−Re(1)−N(4) | 168.6(4) | C(22)−Re(2)−N(3) | 103.7(3) |
| C(25)−Re(1)−N(4) | 94.7(3) | C(21)−Re(2)−N(3) | 164.6(4) |
| C(24)−Re(1)−N(1) | 97.4(3) | C(20)−Re(2)−N(5) | 84.2(4) |
| C(23)−Re(1)−N(1) | 102.8(3) | C(22)−Re(2)−N(5) | 173.9(4) |
| C(25)−Re(1)−N(1) | 168.4(3) | C(21)−Re(2)−N(5) | 98.5(3) |
| N(4)−Re(1)−N(1) | 73.8(3) | N(3)−Re(2)−N(5) | 73.8(3) |
| C(24)−Re(1)−Br(1) | 177.2(3) | C(20)−Re(2)−N(6) | 173.2(4) |
| C(23)−Re(1)−Br(1) | 90.4(3) | C(22)−Re(2)−N(6) | 90.7(4) |
| C(25)−Re(1)−Br(1) | 91.5(3) | C(21)−Re(2)−N(6) | 97.0(4) |
| N(4)−Re(1)−Br(1) | 78.5(2) | N(3)−Re(2)−N(6) | 70.7(3) |
| N(1)−Re(1)−Br(1) | 85.30(19) | N(5)−Re(2)−N(6) | 93.7(3) |
| O(7)−C(3)−N(3) | 112.7(8) | O(7)−C(3)−C(14) | 107.3(7) |
| O(7)−C(3)−N(1) | 110.3(7) | N(3)−C(3)−C(14) | 103.1(7) |
| N(3)−C(3)−N(1) | 112.3(7) | N(1)−C(3)−C(14) | 111.0(8) |

functions as a mixed tridentate-bidentate ligand to two rhenium(I) centers. The slightly distorted octahedral geometry of Re(1) center is defined by a bidentate coordination set of TPT and two carbonyl groups in the equatorial plane; the bromide and the trans carbonyl group assume the axial positions. The least-squares plane through the atoms N(1), N(4), C(23), and C(25) (best plane) about Re(1) shows slight tetrahedral bias with an average deviation of ±0.079 Å, while the deviation of Re(1) from the plane is 0.117 Å. The pyridyl ring containing C(4)−C(5)−C(6)−C(7)−C(8)−N(4) is rotated with respect to the triazine ring by 13.2°.

The tridentate mode of the intact TPT ligand exhibits characteristic coplanarity of the two coordinated pyridyl rings and the central triazine ring with the three nitrogen atoms lying within the equatorial base.[41] However, due to the facial configuration of $Re(CO)_3^+$ moiety, the pyridyl group on the $sp^3$-hybridized C(3) is tilted to such an extent that it is almost perpendicular to both the central triazine ring (90.9°) and the other pyridyl group (84.3°). The highly distorted octahedral geometry around Re(2) is defined by N(5), N(6), C(20), and C(22) in the equatorial plane and N(4) and C(21) occupying the axial positions. The basal plane exhibits tetrahedral bias (average deviations ±0.023 Å), and the out-of-plane distance of Re(2) to the least-squares plane is 0.095 Å. The source of the distortion, as in **7**, is the constraint of the formation of five membered chelate rings; the bites, N−Re−N, shown by the TPT ligand [N(3)−Re(2)−N(5) and N(3)−Re(2)−N(6) of 73.8 and 70.7°, respectively] are significantly smaller than the ideal value of 90°. The rhenium to central N atom distance [Re(2)−N(3)] is shorter, while rhenium to the tilted pyridyl nitrogen distances are longer, than normal rhenium(I) imine nitrogen distances.

## Conclusions

Simple synthetic procedures have been developed to prepare dinuclear rhenium(I) tricarbonyl halide complexes of intact and methoxylated 2,4,6-tris(2-pyridyl)-1,3,5-triazine (TPT) ligand in excellent yield. An unexpected dinuclear Re(I) complex with the methoxylated TPT bridge functioning in a tridentate−bidentate coordination mode to two metal centers has also been isolated in fairly good yield. Although free triaryl-substituted triazines are stable toward nucleophilic attack, coordination of TPT with rhenium(I) resulted in the methoxylation of the ligand in the presence of methanol. After coordination of the ligand to metal ions, the ligand-to-metal $\sigma$-donation and the $\pi$-back-bonding ability of the $d^6$ rhenium(I) metal ions lead to destabilization of the triazine ring enhancing the electron deficiency which makes the carbon atom adjacent to the uncoordinated pyridyl group susceptible to nucleophilic attack, as in the addition of methanol. The addition of $MeO^-$ to C(3) produces tetrahedral geometry around the $sp^3$-hybridized carbon atom. The protonated free pyridyl ring is rotated to such an extent that it is almost perpendicular to the plane of the pentadienide anionic central plane, whereas, for the uncoordinated pyridyl ring in the intact TPT bridged dinuclear complexes, the torsion angle between this pyridyl ring and the triazine is less than 70°. The consequences of tetrahedral geometry and rotation of the pyridyl ring upon addition of methanol are to provide sufficient relief of the steric hindrance to stabilize these methoxy-substituted complexes. Attempts to substitute ethanol, *n*-propanol, or 2-propanol at C(3) proved unsuccessful under similar reaction conditions. This observation may be due to the steric overcrowding of the two coordinated metal center on either side of the carbon atom and to the presence of the pyridyl group which do not allow nucleophilic attack by groups larger than methoxy. The methoxylation did not occur in mononuclear rhenium(I) complexes, which can be

(41) Arif, A. M.; Hart, F. A.; Hursthouse, M. B.; Thornton-Pett, M.; Zhu, W. *J. Chem. Soc., Dalton Trans.* **1984**, 2449.

easily understood by the fact that one metal ion may not be sufficient to make C(3) electropositive ($C^{\delta+}$) enough to encourage nucleophilic attack. Most strikingly, prolonged reaction time and heating in benzene resulted in the elimination of HBr from the complex and the formation of an unprecedented complex **7**. Because the three carbonyl groups have to take a facial configuration, it is impossible to have the pyridyl group attached to the $sp^3$ carbon C(3) simultaneously coplanar to the central methoxylated triazine moiety and the other pyridyl group bound to the same metal. Thus, the pyridyl group adjacent to C(3) is rotated to such an extent that it is almost perpendicular to the other two rings in the coordination environment of the same rhenium metal ion. Mononuclear complexes are usually encountered when the TPT ligand functions as a planar tridentate ligand; however, the single bond character of C(3) decreases the angular strain of the tridentate coordination mode so drastically as to facilitate the presence of two Re(I) in a highly distorted ligand environment.

**Acknowledgment.** This work was supported by a grant from the Department of Energy (DOE), Office of Health and Environmental Research, No. D2-FG02-99ER62791.

**Supporting Information Available:** X-ray data in the form of CIF files and the variable-temperature $^1H$ NMR of complex **7**. This material is available free of charge via the Internet at http://pubs.acs.org. All atomic and thermal parameters and all interatomic angles are available from the author upon request. Crystallographic data (excluding structure factors) for the structure reported in this paper have been deposited with the Cambridge Crystallographic Data Center as publication No. CCDC-143294 to CCDC-143301. Copies of the data can be obtained free of charge on application to CCDC, 12 Union Road, Cambridge CB21EQ, U.K. (e-mail: deposit@ccdc.cam.ac.uk).

IC000446G